Engineered Science
DOI: https://dx.doi.org/10.30919/es951

Noise Reduction in a Bird Inspired Aero Foil using Trailing-Edge Serrations

Shiva Prasad Uppu[1, 2,#,*] and R. Naren Shankar[1,#]

Abstract

The current work deals with the efficacy of the bionic-inspired airfoil of Tyto Alba (a barn owl) in noise reduction. Due to their distinct wing morphology, owls are noted for their quiet flying, which is astonishingly low-noise both when gliding and flapping. The low-noise operation of airfoil is inspired by these remarkable characteristics of owl flight. Research conducted in the past suggests that an airfoil that has an extensive sinusoidal profile can only reduce noise to a certain extent. As a coupling element, an owl-wing-inspired ridge is added to the trailing edge of airfoils with serrations in this work. This proposed method of noise reduction using trailing edge serrations showed the efficacy of a bionic-inspired airfoil with the existing approaches. A numerical study was performed using computational tools and has shown that the proposed bionic-inspired structure could reduce noise more effectively. The results show that wide wavelengths have less low-frequency tonal noise but more at high frequencies. This paper concludes that owl-inspired trailing edge serrations may be an effective aero-acoustic control device for wind turbines, aircraft, drones, and other fluid machines.

Keywords: Acoustics; Frequency; Noise reduction; Owl wing inspired Airfoil; Serrated wing; Sound pressure level.
Received: 16 June 2023; Revised: 17 August 2023; Accepted: 23 August 2023.
Article type: Research article.

1. Introduction

During the past few decades, aircraft have been studied for their aerodynamic performance. It is also an important research topic to study the aerodynamic noise from these practical applications. Airfoils are the base of blades as well as the topic of noise reduction studies.[1,2] Hence, it is of typical interest to study flow noise around airfoils. Traditional passive and active noise reduction techniques have made significant progress, but their application conditions and aerodynamic performance have deteriorated.[3,4] So, there is an urgent need to reduce noise in aerofoils with a novel design. The current advanced design of an airfoil uses noise as one of the critical design indicators.

Bionic design reduces noise by developing and inheriting organism-specific structural traits.[5] Nature blocks sounds. Noise-reducing bionic constructions have been investigated using the owl's quiet flight. Birds' silence affects aerodynamic noise reduction. Many people have studied owl and eagle feathers.[5,6] Velvety fluff, comb-like leading edges, and fringe-like trailing margins allow owls to fly quietly. Regardless of how these wing parts reduce noise, Noise-reduction solutions could use a live owl's aeroacoustics and silent flight. Straight-cut airfoils form a horseshoe vortex.[7] Sawtooth or upwash/downwash flows between serrations make noise. Flow and serration size affect low-frequency tone noise.[8] Woven wire mesh serrations, microscopic brush bundles, synthetic foams, and porous metal reduce tone, according to Ref. [9] Narrow-band tone and broad-band self-noise are reduced in frequency and loudness. This research compares experimental acoustic and flow data for two serration geometries at 40m/s with the LES turbulence model noise prediction using Howe's theory. Varying serration geometry affects trailing edge noise production.

2. Methodology

2.1 Proposed bionic model

In the proposed work, an owl *(Tytus alba)-inspired* aerofoil is introduced for noise reduction. The Primary remiges of the owl wing mimic the leading-edge serrations, and the secondary edges mimic the trailing-edge serrations. The Bionic model of an owl's wing is shown in Fig. 1.

[1] *Department of Aeronautical Engineering, Vel Tech Rangarajan Dr. Sagunthala R&D Institute of Science and Technology, Chennai 600062, TN, India*
[2] *School of Engineering, Ajeenkya D Y Patil University, Lohegaon, Pune 412105, MH, India*
[#] *These authors contributed to this work equally.*
**Email: shivaprasad047@gmail.com* (Prasad U.S.)

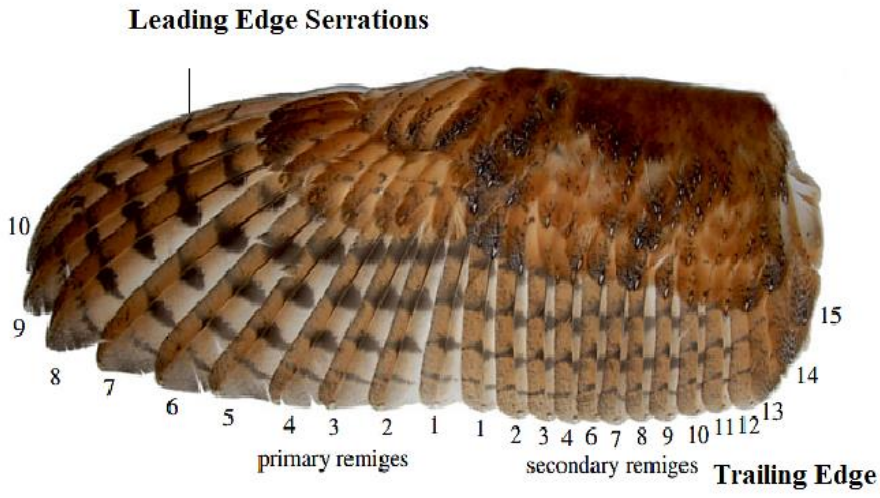

Fig. 1 Owl wing feather indicating feathers and edges. Reproduced with the permission from [10], Copyright 2017 Anatomical Society.

After reconstruction of the bionic model based on Liu and Liao's investigations,[11,12] a bionic aircraft airfoil may be extracted at the 40% spanwise point of the wing model. The measurements and reconstruction of a bionic-inspired owl wing are the focus of these investigations. The thickness distribution and camber line are added and subtracted to describe an airfoil profile[6,13] as presented in Eq. (1).and Eq. (2).

$$D_u = d_c + d_t \quad (1)$$

$$D_l = d_c - d_t \quad (2)$$

D_u is upper surface distribution; D_l is lower surface distribution; d_c is camberline distribution; d_t is thickness distribution is given in Eq. (3).

$$\frac{d_c}{c} = \frac{d_{c(max)}}{c}\eta(1-\eta)\sum_{n=1}^{3} S_n\,(2\eta-1)^{\eta-1} \quad (3)$$

Fig. 2 Front view of bionic inspired wing end view.

In the proposed method a symmetric airfoil (NACA 0012) with 330 mm as chord length is employed and analyzed. Fig. 4 shows the airfoil model components with three trailing edges:

- One without serrations
- Two with cut-out serrations

Both of these cutting serrations possess a 30-mm amplitude root-to-peak and provide better structural integrity and

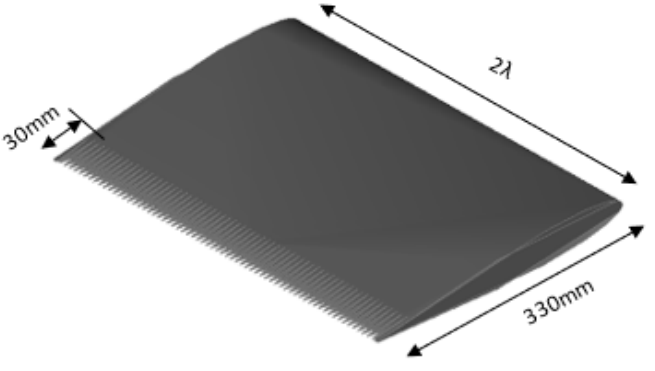

Fig. 3 Isometric view of proposed wing.

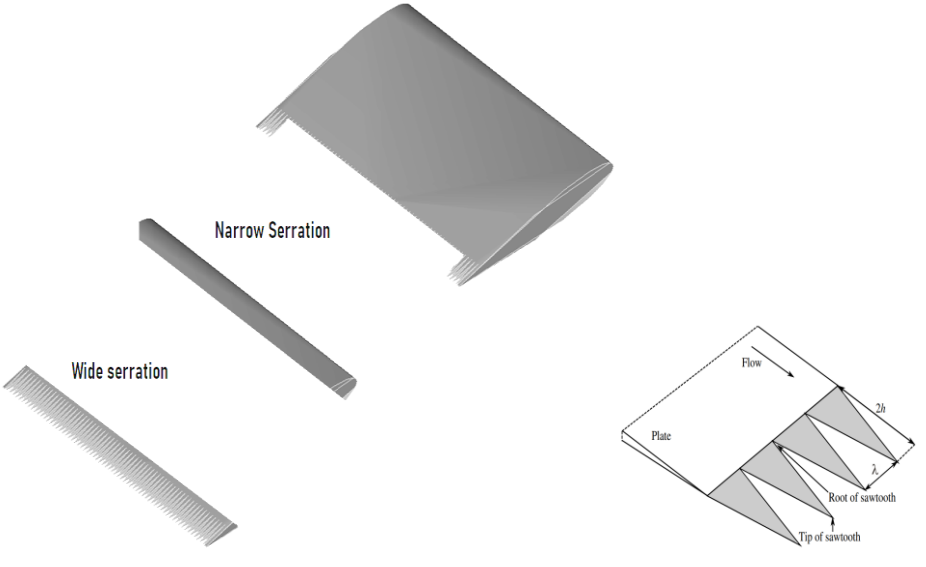

Fig. 4 Illustration of NACA 0012 airfoil with trailing edges serrations.

strength.[14] The study compares two different wavelengths of serration: with λ=6 mm (also called wide serrations or λ6H30, serrated design 1) and λ=12 mm (narrow serrations λ12H30, serrated design 2).

2.2 Mesh and computational setup

An unsteady flow with a velocity of 40 meters per second travelled over the NACA 0012 aerofoil with a chord of 330 millimetres and a span of 2 degrees in a numerical analysis at a 0-degree angle of attack. Transient flow analysis to account for unsteadiness by modifying the LES turbulence model and grid-dependent research with 0.8 million and 2.5 million cells to evaluate flow quality in relation to the grid were successful. Figs. 5a and 5b demonstrate the calculation domain mesh modelling with surface mesh over the airfoil model. The Courant-Friedrichsen-Lewy (CFL) scale measures time numerically. 30 kHz for 0.1 second (50 flow crossings) measures the airfoil's surface pressure. The estimated fields are spatially averaged along the top, bottom, and spanwise directions due to serration flow periodicity. The computational setup replicates the experimental setup, which measures far-field noise using an isolated microphone (GRAS-46AE).[13] The microphone is 1.5 meters from the platform. The experimental arrangement is shown below:

Sound pressure levels are sampled at Baseline, 6H30, and 12H30 with different sampling frequencies. For the selected frequencies, the minimum at baseline is 140.99 Hz, and the maximum at baseline is 4014.91 Hz. The lowest, at Baseline, and highest sound pressures are 67.00 Hz, and the maximum is 55.13 Hz. Noise data is obtained by using a computational tool with a large eddy simulation model in the frequency range of 100 Hz to 100 kHz for 150 seconds. SPL for One third-octave is extracted at 1.5m above the serration of the wing, and seven receivers are placed over the serration edge to capture the SPL effectively. Experimentally, a 4014 data set point window size was used, whereas in the current work, data is extracted over the serration at the centerline of the wing and in between the serrations. At an angle of attack (α= 0°), Acoustic data is obtained at a speed of V∞ = 40 m/s.

3. Results

3.1 Baseline and serrated design analysis

The SPL data is compared with the baseline experimental data and serrated wing data provided in the proposed study, which correspond to the condition where the main body of the NACA 0012 airfoil has an unserrated trailing edge.[15] Fig. 6 shows the SPL plot for this scenario at various flow rates that are compared with experimental data. The NACA 0012 airfoil

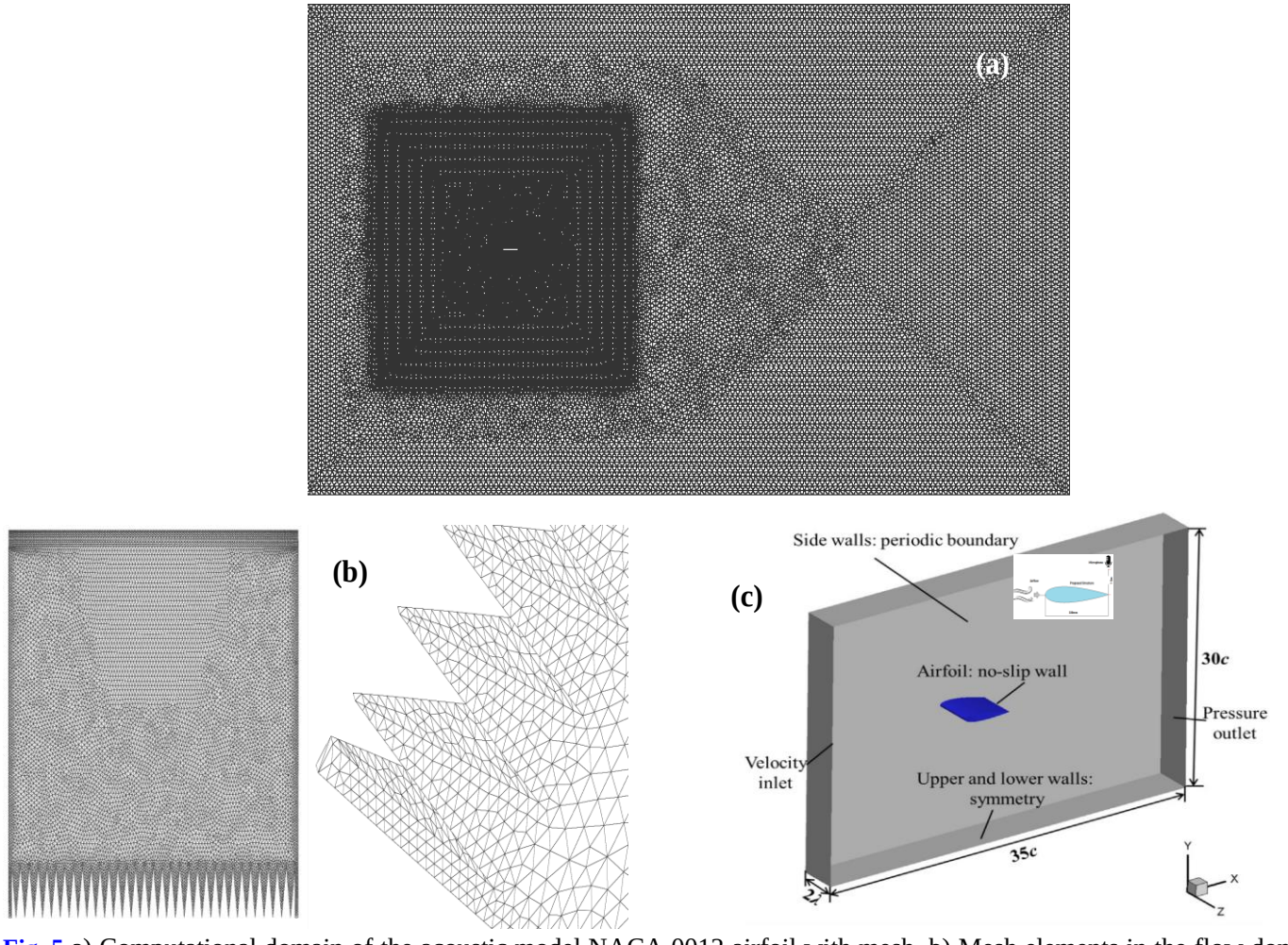

Fig. 5 a) Computational domain of the acoustic model NACA 0012 airfoil with mesh, b) Mesh elements in the flow domain with an explored view of the airfoil and surface mesh, c) Numerical setup.

generates broadband self-noise at the tested flow speeds of 40 m/s, as shown in Figs. 6 and 7.

An Analysis Fig. 6 depicts serrated design 1, with noise-based serrated trailing edges at V = 40 m/s. Several previous observations have found high frequencies.[14] Above the baseline, these additional serrations result in the amplification of low-frequency narrow-band noise, which adversely impacts the reduction of noise. As flow speed increases, there is an increase in Low- frequency tonal noise, while the number of serrations decreases with wavelength.

Based on the trailing edge serration bluntness and the Strouhal number $St = f/V_\infty$, Fig. 6 illustrates the difference in △SPL. That is between the experimentally recorded data and numerically determined trailing edge serration sound pressure level data. In △SPL, the positive value corresponds to increased noise, whereas the negative value corresponds to reduced noise. The spectral hump is seen to collapse into nearly constant $St = f/V_\infty$ values as the flow speed changes. As a result, tonal noise arises from the vortices in the serrations. Because wide serrations reduce broad-band noise more at mid frequencies than narrow serrations, while the latter raise low and high-frequency noise less, the former reduces broad-band noise more at mid frequencies. Serrations with wide serrations surpass serrations with narrow serrations.

The sound pressure level for serrated design 1 is represented in Fig. 6. Frequency is represented in the x axis and the y axis by SPL. The sound pressure level for serrated designs reaches its peak at 67 dB at 2000 Hz for computational data. While for experimental data, the sound pressure level for a serrated design reaches its peak at 64 dB at 2000 Hz.

Serrated design 2 sound pressure level is represented in Fig. 7. Frequency is represented in the x axis and the y axis by SPL. The sound pressure level for serrated designs reaches its peak at 67 dB at 2000 Hz for computational data. While for experimental data, the sound pressure level for a serrated design reaches its peak at 65 dB at 200 Hz. The SPL of Computational and Experimental data is the same and merges at 10 kHz. The plots in Figs. 6 and 7 show that the calculated findings agree well with the experimental data, indicating that the computational method has reliably forecast the experimental results.

The sound pressure level for receivers located at different locations as presented in Table 1 is indicated as R1, R2, R3, R4, R5, R6, R7, R8. serrated design 2 is represented in Fig. 8. Frequency is represented in x axis is and y axis is SPL. The sound pressure level for serrated design reaches is maximum at R2 and R6 above 110dB and R4 at 1kHz. The sound pressure level decreases on increasing frequency. The SPL is minimum at 10kHz.

The sound pressure level for (R1, R2, R3, R4, R5, R6, and R7) serrated design 1 is represented in Fig. 9. Frequency is represented in the x axis and the y axis by SPL. The sound pressure level for serrated designs reaches its maximum at R2 110 dB, R6 109 dB, and R4 50 dB at 1 kHz. The sound pressure level decreases with increasing frequency. The SPL is decreasing with an increase in frequency level, as presented.

Airfoil data for two serrated variants of the NACA 0012 airfoil was developed using a Large Eddy Simulation (LES) model with unsteady flow analysis as presented in Fig. 10. The vortex model sheds the airfoil. Thus, quiet owl flight research

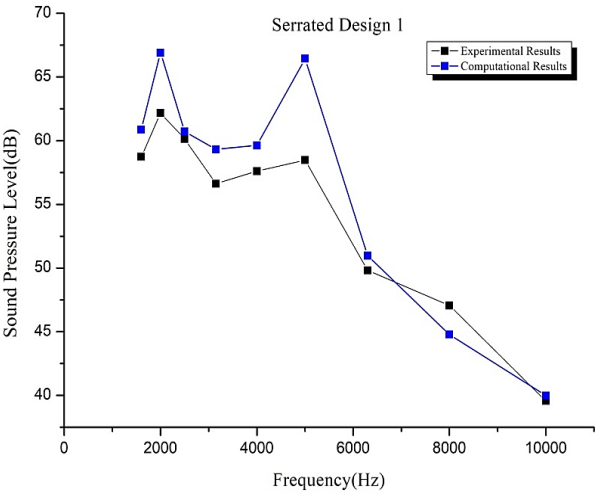

Fig. 6 Sound pressure level of Serration design 1.

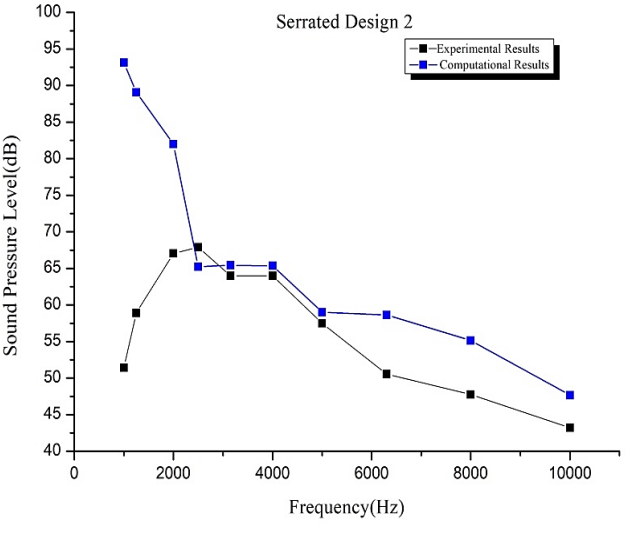

Fig. 7 Sound pressure level of Serration design 2.

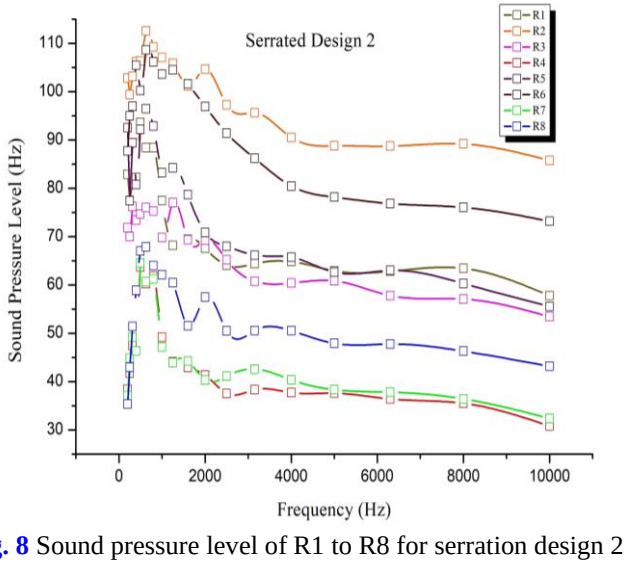

Fig. 8 Sound pressure level of R1 to R8 for serration design 2.

Table 1. Receiver location at the trailing edge of wing.

Receiver Name	X(m)	Y(m)	Z(m)	Serration design 1 (OASPL)dB	Serration design 2 (OASPL)dB
R1	0.266	0.0047	0.199	100.263	99.0649
R2	0.273	0.0038	0.199	137.857	100.277
R3	0.280	0.0029	0.199	114.541	115.648
R4	0.287	0.0020	0.199	119.127	113.008
R5	0.294	0.0012	0.199	115.303	86.341
R6	-0.560	1.2287	0.202	67.2802	72.4444
R7	1.160	1.2287	0.202	66.7925	72.163
R8	0.300	1.5	0.199	69.7962	74.8663

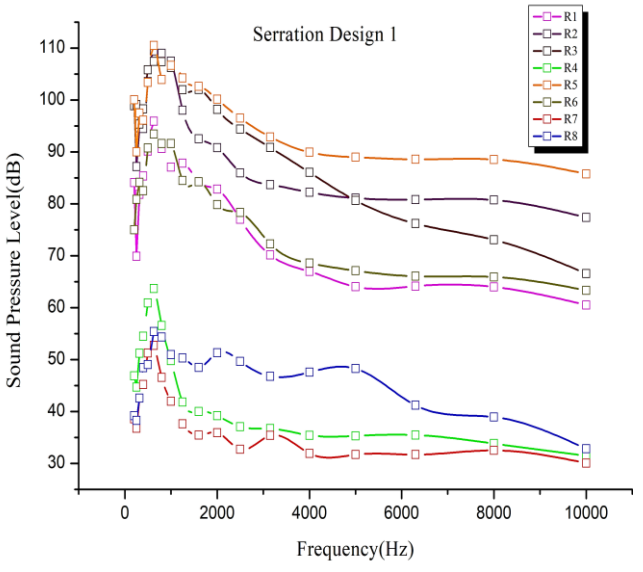

Fig. 9 Sound pressure level of R1 to R8 for serration design 1.

could lead to a new biomimetic design or noise reduction technology for wind turbine blades or rotors, airplanes, and multi-rotor drones. Wind turbine blades and rotors could benefit from biomimetic design or noise reduction technologies. In order to evaluate computational tools, a study was conducted to validate the results using coefficients of lift and drag data over dimensionless time. The variation of coefficients with respect to time is in the range of 0.0075 to 0.01 for the serrated design 2, and the coefficient of list was close to zero in both the design evaluations of the NACA 0012 wing with serrations.

Figure 11 represents the coefficient of lift of a serrated design 2 aerofoil, where the X axis is time and the Y axis is Coefficient of lift. that is increasing at 20 s, reaching a maximum at 60s, and again at 150 s. Fig. 12 represents the Coefficient of lift of the serrated design 1 NAC0012 foil. Where X is time and Y is the coefficient of lift. C_l Gradually increases at 20 s and reaches its peak at 80 –100 s. Fig. 13

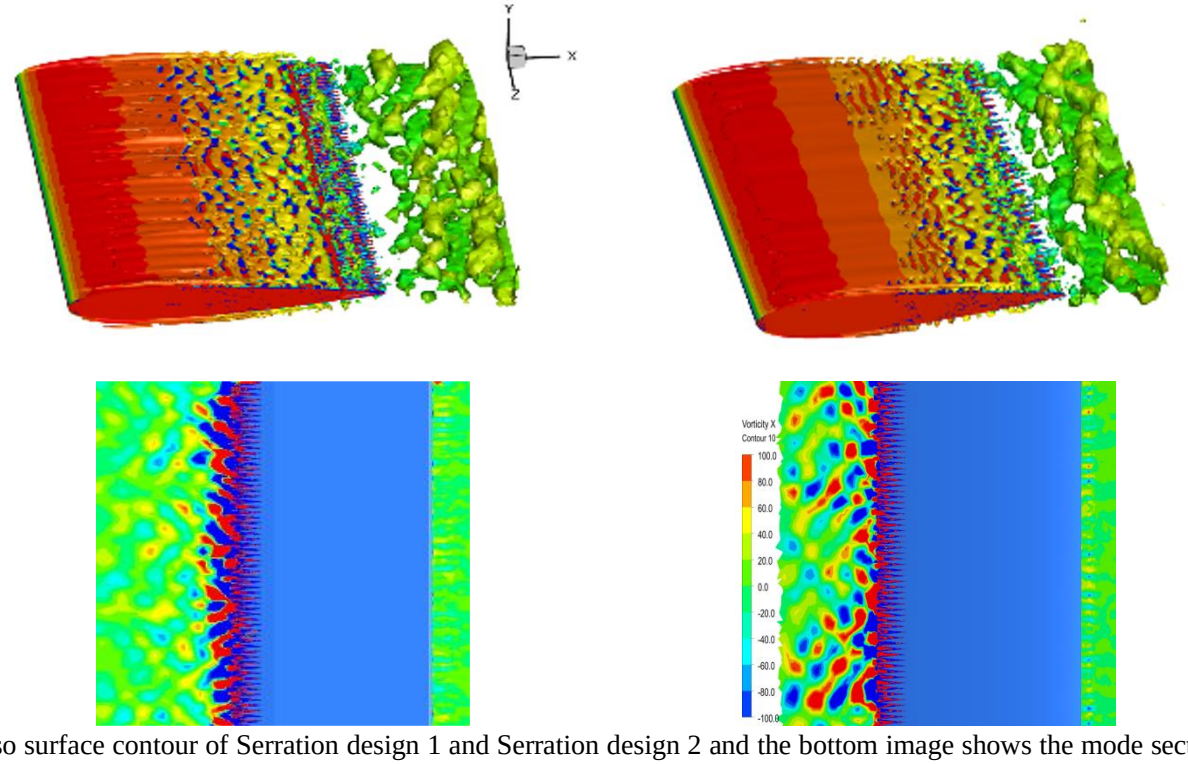

Fig. 10 Iso surface contour of Serration design 1 and Serration design 2 and the bottom image shows the mode section along the centerline of the plan view showing the vortex shedding over the airfoil.

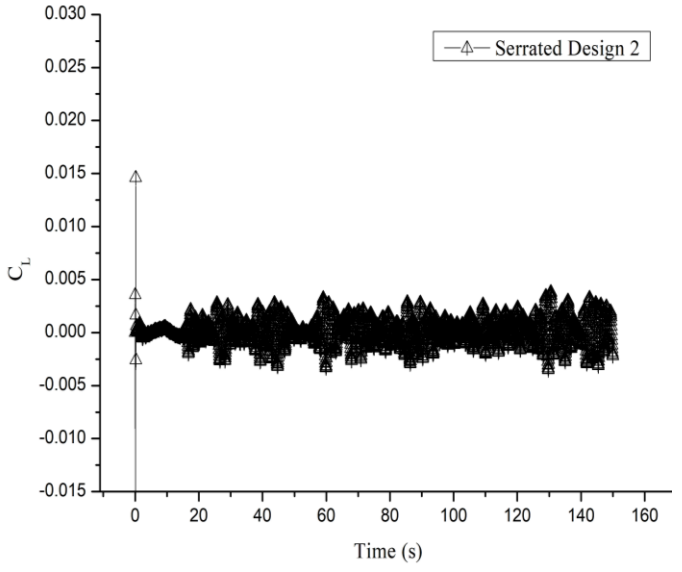

Fig. 11 Coefficient lift for serration design 2.

represents the coefficient of drag of the serrated design 2 aerofoil, where the X axis is time and the Y axis is Coefficient of drag. The C_D 0.007 declines at 10s and steadily progresses till 110, then again elevates a little 0.08 C_D and progresses steadily till 160 s. Fig. 14 represents the coefficient of drag of the serrated design 1 aerofoil, where the X axis is time and the Y axis is Coefficient of drag. The C_D 0.001 declines from 0 to 10s and steadily progresses until 160 s.

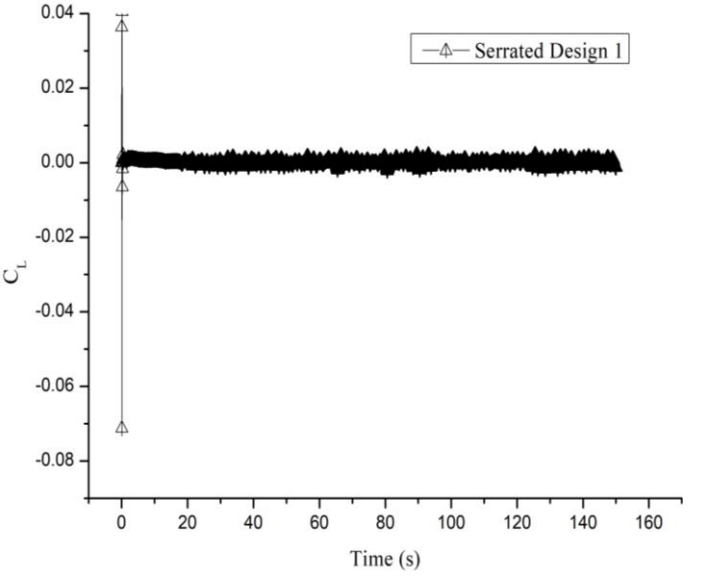

Fig. 12 Coefficient lift for serration design 1.

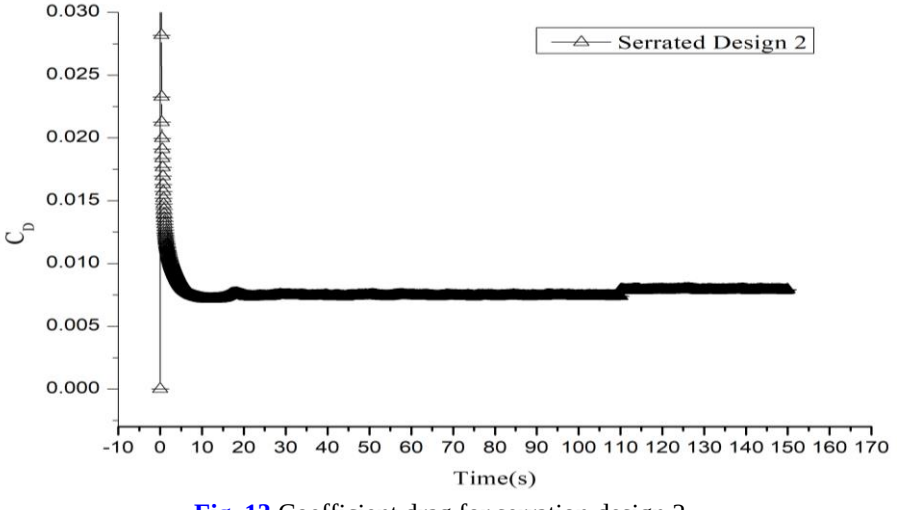

Fig. 13 Coefficient drag for serration design 2.

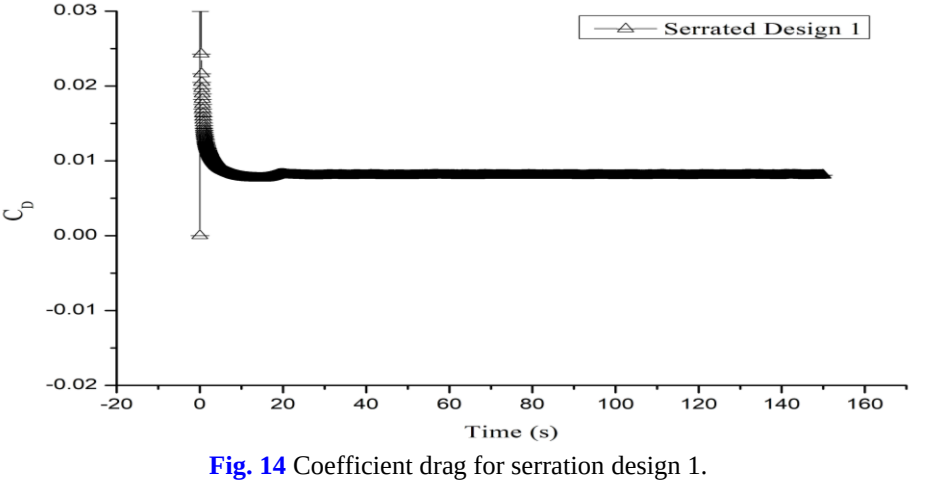

Fig. 14 Coefficient drag for serration design 1.

4. Conclusions

We investigate the applicability of LES for modelling both types of toothed wings. Serrations on the trailing edge of a bionic-inspired airfoil have been shown to reduce noise significantly. Compared to narrow serration, wide serration is 2 dB more effective at reducing noise in the midrange, according to computational studies. The significance of pressure over the wing is well demonstrated by experimental and computational studies, which concur well. This research was highly sought after by experts, who have long been intrigued by the owl's intricate navigational techniques and stable management of the aero-acoustic environment while flying silently. The sound waves emitted by the various sensors are affected by the pressure differential across the wing's serrations. Lift and drag contribute to the commotion at the serrations on the trailing edge. The noise-cancelling mechanism, the effects of serration width on aerodynamics, the brush's hair and length, and so on, will all be the subject of further study.

5. Future work

This investigation aims to reduce the noise level of the NACA 0012 aerofoil. Unsymmetrical airfoil design options with acoustically optimized wing designs can be the subject of future research. In subsequent studies, the porosity of owl wing membranes can be analyzed and utilized for noise reduction. Future research might include the bird-inspired bionic wing.

Conflict of Interest

There is no conflict of interest.

Supporting Information

Not applicable.

References

[1] Y. Wei, F. Xu, S. Bian, D. Kong, Noise reduction of UAV using biomimetic propellers with varied morphologies leading-edge serration, *Journal of Bionic Engineering*, 2020, **17**, 767-779, doi: 10.1007/s42235-020-0054-z.

[2] M. Zhao, H. Cao, M. Zhang, C. Liao, T. Zhou, Optimal design of aeroacoustic airfoils with owl-inspired trailing-edge serrations, *Bioinspiration & Biomimetics*, 2021, **16**, 056004, doi: 10.1088/1748-3190/ac03bd.

[3] D. Li, X. Liu, F. Hu, L. Wang, Effect of trailing-edge serrations on noise reduction in a coupled bionic aerofoil inspired by barn owls, *Bioinspiration & Biomimetics*, 2019, **15**, 016009, doi: 10.1088/1748-3190/ab529e.

[4] C. Rao, H. Liu, Aerodynamic robustness in owl-inspired leading-edge serrations: a computational wind-gust model, *Bioinspiration & Biomimetics*, 2018, **13**, 056002, doi: 10.1088/1748-3190/aacb43.

[5] L. Wang, X. Liu, D. Li, Noise reduction mechanism of airfoils with leading-edge serrations and surface ridges inspired by owl wings, *Physics of Fluids*, 2021, **33**, 015123, doi: 10.1063/5.0035544.

[6] H. Wagner, M. Weger, M. Klaas, W. Schröder, Features of owl wings that promote silent flight, *Interface Focus*, 2017, **7**, 20160078, doi: 10.1098/rsfs.2016.0078.

[7] D. J. Moreau, C. J. Doolan, Noise-reduction mechanism of a flat-plate serrated trailing edge, *AIAA Journal*, 2013, **51**, 2513-2522, doi: 10.2514/1.j052436.

[8] D. Li, X. Liu, L. Wang, F. Hu, G. Xi, Numerical study on the airfoil self-noise of three owl-based wings with the trailing-edge serrations, *Proceedings of the Institution of Mechanical Engineers*, *Part G*: *Journal of Aerospace Engineering*, 2021, **235**, 2003-2016, doi: 10.1177/0954410020988229.

[9] A. Vathylakis, T. P. Chong, P. F. Joseph, Poro-serrated trailing-edge devices for airfoil self-noise reduction, *AIAA Journal*, 2015, **53**, 3379-3394, doi: 10.2514/1.j053983.

[10] M. Weger, H. Wagner, Distribution of the characteristics of barbs and barbules on barn owl wing feathers, *Journal of Anatomy*, 2017, **230**, 734-742, doi: 10.1111/joa.12595.

[11] W. Yang, Q. Sai, D. Guo, D. Huang, N. Wang, A bionic approach for axial flow fans to reduce the noise, *Journal of Chinese Society of Power Engineering*, 2022, **42**, 530-536, doi: 10.19805/j.cnki.jcspe.2022.06.006.

[12] J. Wang, K. Ishibashi, M. Joto, T. Ikeda, T. Fujii, T. Nakata, H. Liu, Aeroacoustic characteristics of owl-inspired blade designs in a mixed flow fan: effects of leading- and trailing-edge serrations, *Bioinspiration & Biomimetics*, 2021, **16**, 066003, doi: 10.1088/1748-3190/ac1309.

[13] Y. Wang, Y. Zhao, H. Tian, K. Zhao, Y.-B. Song, Reduction of trailing-edge noise by means of brush-serrated coupling bionic structure, *IOP Conference Series*: *Materials Science and Engineering*, 2019, **538**, 012053, doi: 10.1088/1757-899x/538/1/012053.

[14] Tze Pei Chong, Alexandros Vathylakis, Phillip F. Joseph and Mathieu Gruber, Self-Noise Produced by an Airfoil with Non-flat Plate Trailing-Edge Serrations, *AIAA Journal*, 2013, **51**, 2665-2677, doi: 10.2514/1.J052344.

[15] Y. Wang, K. Zhao, X.-Y. Lu, Y.-B. Song, G. J. Bennett, Bio-inspired aerodynamic noise control: a bibliographic review, *Applied Sciences*, 2019, **9**, 2224, doi: 10.3390/app9112224.